Development and application of reservoir models and artificial neural networks for optimizing ventilation air requirements in development mining of coal seams

C. Özgen Karacan

National Institute for Occupational Safety and Health (NIOSH) Pittsburgh Research Laboratory Pittsburgh, PA 15236, United States

Abstract

In longwall development mining of coal seams, planning, optimizing and providing adequate ventilation are very important steps to eliminate the accumulation of explosive methane–air mixtures in the working environment. Mine operators usually try to supply maximum ventilation air based on the capacity of the system and the predicted need underground. This approach is neither economical nor safer as ventilation capacity may decrease in time depending on various mining and coalbed parameters. Thus, it is important to develop better engineered approaches to optimize mine ventilation effectiveness and, therefore, to ensure a safer work environment.

This study presents an approach using coalbed methane reservoir modeling and an artificial neural network (ANN) design for prediction and optimization of methane inflows and ventilation air requirements to maintain methane concentrations below statutory limits. A coalbed reservoir model of a three-entry development section, which is typical of Pittsburgh Coalbed mines in the Southwestern Pennsylvania section of Northern Appalachian Basin, was developed taking into account the presence and absence of shielding boreholes around the entries against methane inflow. In the model, grids were dynamically controlled to simulate the advance of mining for parametric simulations.

Development and application of artificial neural networks as an optimization tool for ventilation requirements are introduced. Model predictions are used to develop, train, and test artificial neural networks to optimize ventilation requirements. The sensitivity and applications of proposed networks for predicting simulator data are presented and discussed. Results show that reservoir simulations and integrated ANN models can be practical and powerful tools for predicting methane emissions and optimization of ventilation air requirements.

Keywords: Underground mining; Coalbed reservoir modeling; Artificial neural networks; Mine ventilation; Reservoir simulation; Mine safety

1. Introduction

In development mining, continuous advance of mine workings may cause variations in the amount and rate of methane emissions into the mine atmosphere, which leads to ventilation requirements continuously changing to maintain gas levels below legal limits. If adequate ventilation is not provided, this condition can result in elevated methane concentrations, which can increase the risk of an explosion or a frictional ignition that may lead to an explosion. In order to improve the safety of underground coal mines, it is important to have the predictive capabilities to estimate methane emission

rates based on coalbed and mining parameters at a particular stage in mining and to be able to optimize the mine ventilation requirements.

In addition to improved worker safety, optimization of ventilation air requirements can also provide a cost benefit. Historically, mines tended to supply a fixed volume of air based on the projected maximum demand (Hardcastle et al., 1997). In today's economic environment, ventilation can consume 30–40% of the electricity used in underground coal mining operations. It is important to optimize the ventilation requirements to reduce the ventilation costs in underground coal mines.

As development mining progresses, entry length and the number of cross cuts (leakage) increase, requiring additional airflow to adequately ventilate the work areas. Furthermore, as development lengths increase, it may become increasingly difficult to keep methane levels under statutory limits by ventilation alone. One of the most effective approaches to drain excessive methane from the coalbed before mining starts and to shield the entries against methane inflow (Brunner et al., 1997; Noack, 1998; Diamond, 1994) is to drill horizontal boreholes in the coalbed. This approach has been proven to be very effective. Horizontal drilling technique and its application to degasify coal seams are documented in the literature (Thakur and Davis, 1977; Thakur and Poundstone, 1980; Thakur, 1997). However, no predictive techniques and guidelines exist that establish the distance between the entries and horizontal wells for optimal shielding and to detail the timing between well drilling and development mining for optimal degassing of the coal.

It is important to improve predictive and optimization methods to provide adequate ventilation air based on the coalbed and mining parameters. Over the years, reservoir-modeling methods and simulators have been developed that can realistically represent the complex physics of reservoir flow mechanisms in coalbeds and gas production operations with diverse well completions (King and Ertekin, 1991). These simulators have been successfully applied in various coal basins for coalbed gas recovery using both vertical and horizontal boreholes (Ertekin et al., 1988; Zuber, 1998; Young et al., 1993). These models offer advanced predictive capabilities to simulate the development mining process and the prediction of methane inflow rates (Zuber, 1997) as well as the subsequent determination of airflow requirements based on coalbed and mining parameters. However, as the number of independent variables increases, model solution and analysis become increasingly difficult.

Artificial neural networks (ANNs), on the other hand, are adaptable systems that can determine relationships between different sets of data. ANNs have been developed to solve problems where conventional computer models are inefficient. These problems are either non-polynomial types having no polynomial relationship or very complex problems that are difficult to describe mathematically. The key advantages of neural networks are their abilities to learn, to recognize patterns between input and output space, to generalize solutions, and to interpret incomplete and noisy inputs. Statistical techniques such as multiple regression analysis have been used widely for these kinds of problems, but they often fail in accuracy of prediction, especially in the face of highly non-linear relationships or incomplete and noisy data. Owing to the massively parallel, distributed processing nature of ANNs that can improve their ability through dynamic learning, they may outperform other methods of prediction and optimization. Due to their inherent capabilities and flexibilities, artificial neural networks are a powerful predictive and optimization method when used in conjunction with reservoir simulation methods for predicting methane inflow and optimizing ventilation requirements during development mining.

2. Objective and description of the study

This paper presents the development and application of reservoir simulation and artificial neural network models for improved prediction and optimization of methane inflow rates and ventilation requirements during development mining sections in coal seams. The reservoir models were developed based on a typical three-entry Pittsburgh Coalbed mine operating in the Southwestern Pennsylvania section of the Northern Appalachian Basin. These models were constructed with and without the presence of degasification and shielding against methane. They were developed using Computer Modeling Group's (CMG, 2003) compositional reservoir simulator (GEM). The models were run "dynamically" to simulate advance of entry development using a "restart" approach (Karacan et al., 2005, in press). The reservoir model predictions were compared with the in-mine monitoring data of air quality and flow rate obtained during tailgate and headgate entry development around a longwall panel. Various mining and degasification-related parameters were considered for parametric runs using this reservoir simulator.

The "synthetic" cases generated while performing reservoir simulation runs were used to develop, train, and test the artificial neural network (ANN) models, which were developed using Neurosolutions 5.0 software (NeuroDimensions, 2006). The proposed ANN models

were evaluated for their learning and predictive performances of reservoir simulation results.

3. Reservoir-modeling approach to simulate development mining

3.1. The mining site monitored for model comparisons

For modeling development mining, a three-entry tailgate and headgate development, typical of coal mines operating in Pittsburgh Coalbed in the Southwestern Pennsylvania section of the Northern Appalachian Basin, was analyzed (Fig. 1).

During the mining of headgate and tailgate entries, ventilation air qualities and flow rates were measured by the operating mining company using methanometers and flow meters at the monitoring locations shown in Fig. 1. Methane inflow rates were quantified based on the measured data. The data was reported as average monthly concentrations of methane, airflow rate, raw and clean tonnages of produced coal, and total linear distances advanced during mining. The length of each entry section was around 11,000 ft (3353 m) and took 8–9 months to mine.

3.2. Coalbed reservoir and modeling parameters

The base model for formulating development mining was a coalbed methane reservoir model. A single-layer coalbed reservoir model was created in Cartesian coordinates to model fluid flow in the unmined sections of the coalbed and in the entries, as well as to simulate development mining operation. In the development of the model, the parameters and their average values in Table 1 were used for the Pittsburgh Coalbed. The data for pre-mining reservoir properties were gathered from previous NIOSH publications, external reports, personal communications with the operating mining company, and previous history matching studies (Karacan et al., 2005, in press).

Table 1
Values of some of the reservoir parameters of Pittsburgh Coalbed used in the models

Parameter	Value
Permeability-face cleat (md)	4
Permeability-butt cleat (md)	1
Effective porosity (%)	4
Effective fracture (cleat) spacing (ft)/(m)	0.1/0.03
Langmuir pressure (psi)/(MPa)	326/2.25
Langmuir volume (scf/ton)/(cc/g)	490/15.5
Desorption time (days)	20
Initial water saturation (%)	60
Coal density (lb/ft^3)/(g/cc)	84.7/1.35
Pressure (psi)/(MPa)	90/0.61

In the Pittsburgh Coalbed in the Central and Northern Appalachian Basin, face and butt cleats are perpendicular and parallel, respectively, to the fold axis. At the study mine, face cleats were oriented in the E–W direction and butt cleats in the N–S direction. This information indicates that the direction of mine advance is parallel to the face cleats and perpendicular to butt cleats. When positioning the simulation grids and assigning the permeabilities, attention was given to cleat directions.

The gas content and adsorption related data for the Pittsburgh Coalbed was obtained from the results of methane adsorption and direct method of gas content determination tests on various coal samples (Diamond et al., 1986) and from an unpublished report of Langmuir parameters of a site-specific core. The spatial distributions of fracture permeabilities of the Pittsburgh Coalbed have not been previously established or reported. However, based on a large scale modeling study involving estimation of some coalbed parameters (Karacan et al., 2005, in press), the average permeabilities for the Pittsburgh Coalbed were estimated to be 4 md in the

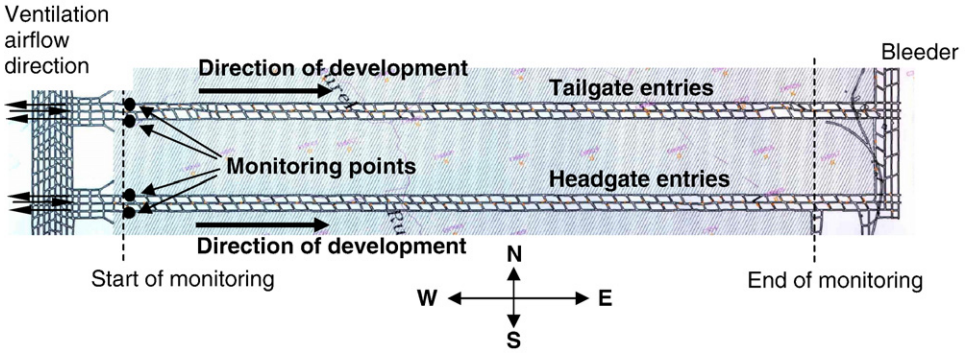

Fig. 1. The modeled long wall panel showing entry sections where mining and ventilation data was gathered during development mining.

Table 2
The parameters and their range of values changed in simulation runs

Parameter	Range
Mining height (ft)/(m)	5–7/1.52–2.13
Entry length (ft)/(m)	1000–12,000/305–3658
Mining rate (ft/day)/(m/day)	25–175/7.6–53.3
Methane concentration in mine air (%)	0.5–1.5
Distance of shielding wells to entries (ft)/(m)	19–87/5.8–26.5
Degasification duration before mining (days)	0–180

face cleat direction and 1 md in the butt cleat direction. In the simulations, these values were taken to be uniform throughout the layer.

The gas relative permeability curve of the coalbed was estimated by matching the average gas production rate from the simulated boreholes in the models to the reported average methane production rates of three horizontal degasification boreholes in the mining area [8.42 scf/day/ft (0.782 m^3/day/m) vs. 8.70 scf/day/ft (0.807 m^3/day/m)]. A similar field-data-based adjustment could not be made to the water relative permeability curve because no data was available. Thus, the curve was set to low values so the wells would experience low amounts of water [0.0016 bbl/day/ft (0.0015 m^3/day/m)].

3.3. Modeling of development mining process and performing the simulations

Various factors control the ventilation requirements during development mining. Among these factors, coalbed parameters and mining parameters are probably the most important. In this study, the Pittsburgh Coalbed was selected as the primary coalbed of interest and its average properties (Table 1) were used in the models. Thus, the variables originating from coalbed reservoir properties were mostly eliminated from parametric runs and subsequent analyses. In that sense, these models may be considered site-specific to Pittsburgh Coalbed. However, the effects of coalbed parameters can be investigated easily using the same approach to increase the predictive capability for other coalbeds. The main areas of emphasis were mining parameters, the methane concentration level to be maintained, and the presence or absence of a degasification/shielding program to reduce the amount of methane emissions into the developed entries. Based on this approach, two different types of models, with and without horizontal degasification wellbores, were developed and simulation runs were performed. The parameters and their ranges of values are shown in Table 2.

For modeling driveage of tailgate and headgate entries, a three-entry development model around a longwall panel was studied. Fig. 2 shows a snapshot of the model that represents mining advance, pillar layout, and the ventilation scheme. An oblique plane was removed from the picture for a better visualization of the different elements of the model. The middle entry was modeled as the "track" or haulage entry, where intake air was entering. In this entry, ventilation air injection and mine pressure assignments to the grids were performed using an injector well. The entry to the left of "track" was designated as the "belt" entry. The third entry was designated as the "return" entry carrying away majority (>90%) of the methane emissions and the methane-loaded ventilation air. The producer wells used in these entries both assigned the mine pressures and monitored the amount of methane in the produced gas stream. This was the amount of methane entering the entries as mining progressed and was used to calculate ventilation requirements to dilute it to desired levels at any stage in mining.

During development mining, the entries and the cross cuts constituting the volume to be ventilated are continuously extended imposing a moving boundary-type problem in modeling. As the continuous miner advances, new volumes are created that must be ventilated while new surfaces are created that liberate gas into that volume. In this study, the development of a three-entry continuous mining model, shown in Figs. 2 and 3, was handled using "restart" model runs. These models were run sequentially, each characterizing an advance in entry development with a specified development rate where coalbed properties were replaced with the assigned properties of the entries in the models and ventilation-related features are built. The simulation

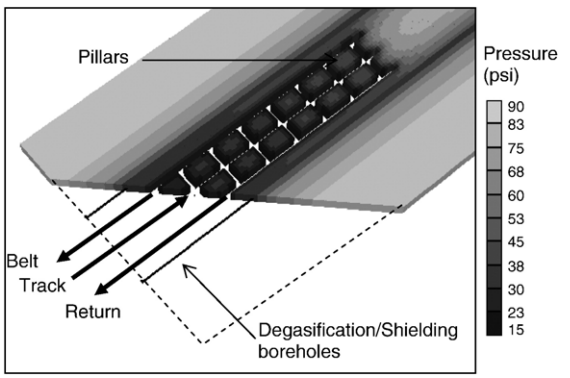

Fig. 2. A three dimensional snapshot of pressure distribution during development of the coalbed. Pillars, ventilation scheme and the modeled shielding wells are also shown.

outputs from the previous model run were written in a "restart" file and then used by the next model as the input run, while reservoir parameters were changed to characterize the development of entries. This approach was used recently by Karacan et al. (2005, in press) to model the longwall mining process and the performances of gob gas ventholes. Zuber (1997) approached the problem of roadway development by using a reservoir simulator and modifying the grids at appropriate times at the differential equation level without restarting the simulation.

In building the restart models, all three entries were developed simultaneously to a specific distance in a predefined amount of time, allowing calculation of the

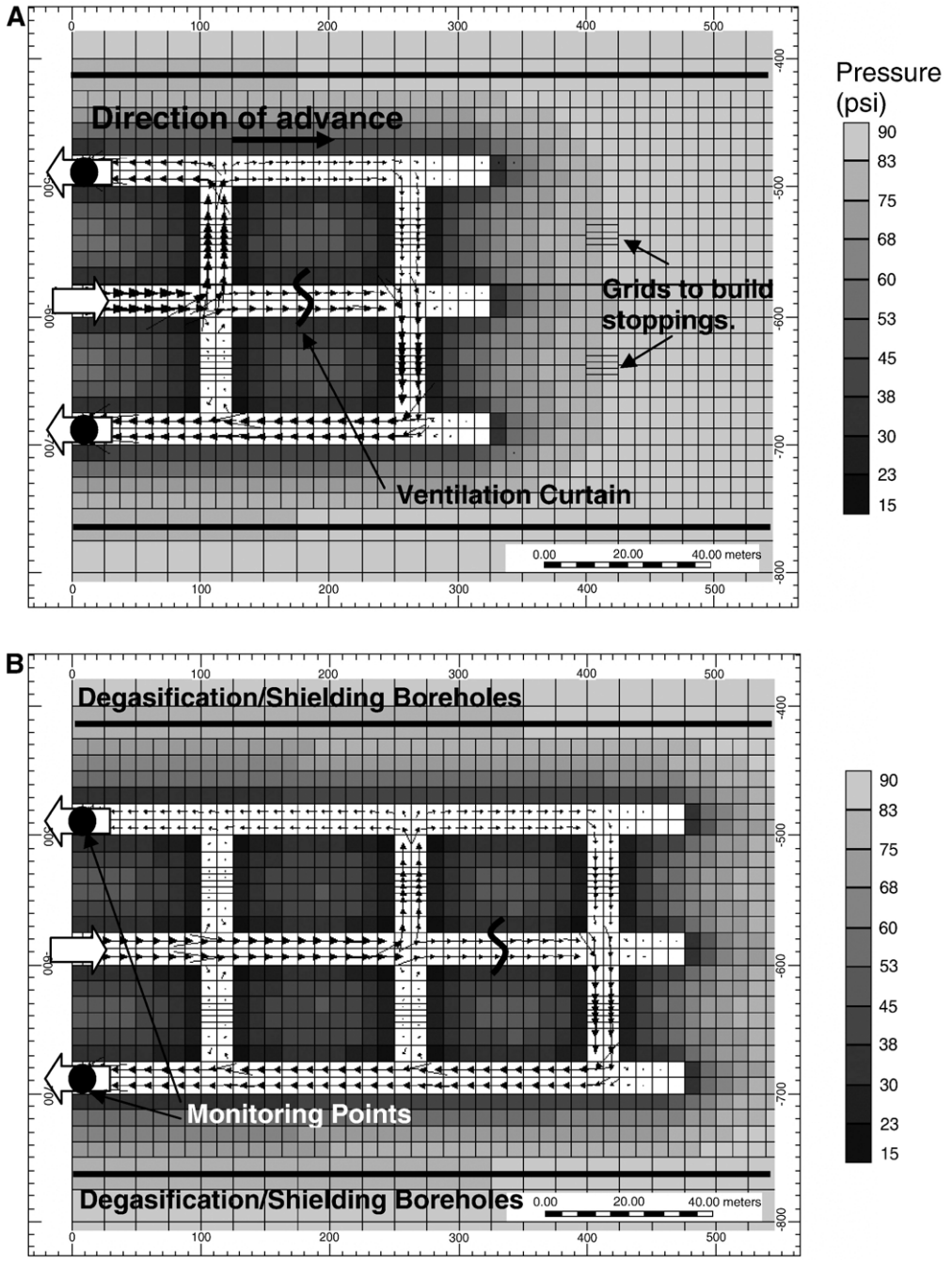

Fig. 3. (A–B) A portion of the grid model showing the advance of mining at two successive stages and the resultant ventilation airflow paths (arrows).

rate of mining advance. For different mining rates, the times in the recurrent data set were changed. Thus, the rates reported in this study are not linear mining rates, but instead represent the rates of the mine section advance. Based on this approach, a 150 ft (45.7 m) section advance corresponds to 570 ft (173.7 m) of linear mining distance in the model, including entries and cross cuts.

As the entries were developed at the designated rates in the models by changing coalbed properties, the pillars and cross cuts were also developed at the same time. The pillars between the entries were 125 ft (38.1 m) in length and 75 ft (22.9 m) in width, and had the same properties as the coalbed. However, during the development of entries, each of which was 20 ft (6.6 m) in width and the same height as the coalbed, the permeability was replaced with a high permeability [10^9 md (10^{-6} m^2)] in all three directions. Also, the coal-matrix pressures in the mined grids were assigned to atmospheric pressures to simulate mining process.

The development of cross cuts was modeled the same way as the entries. However, during each simulation run only the last set of cross cuts was left fully open for ventilation airflow. During the development of cross cuts, stoppings or block walls (between track-belt and track-return) were automatically created between the restart runs to force ventilation flow through the last cross cuts at each section advance. A "curtain" resistance in the last section of the "track" diverted some of the intake air towards the "belt" entry to ventilate both belt and face (Fig. 3A and B). A permeability of 100 md (10^{-13} m^2) was assigned to the stoppings to represent leakage, a common occurrence in underground mining. Fig. 3A and B shows the progress of mining between two successive steps. These figures show the entries, cross cuts, and the pillars created during simulations plus the path of the ventilation airflow.

In this study, two different modeling approaches were undertaken to predict methane inflows and to estimate ventilation requirements during development mining: with and without degasification wellbores around the entries to shield them from migrating methane. The variables of these models were mining rate, mining height (coalbed thickness), methane percentage in the ventilation air, length of developed entries, pre-mining degasification duration and the proximity of boreholes to the entries, as summarized in Table 2. In the models with shielding boreholes, the borehole diameters were 3 in. (7.6 cm), with no wellbore skin, and they were operated with −0.2 psia (−1260 Pa) bottom-hole pressure. The lengths of the boreholes were equal to the lengths of the entries. The wellbores were operated during mining regardless of the duration of the pre-mining degasification period.

4. Analysis of reservoir model predictions of methane inflow and airflow

4.1. Description of mining conditions and parameters in the monitored mine and comparisons with model predictions

During mining of tailgate and headgate entries shown in Fig. 1, various parameters of mining and ventilation were measured by the operating mining company. The linear advance distances, lengths of the exposed ribs, as well as raw and clean coal tonnages were reported as monthly totals. The measured air quality, ventilation airflow rates, and calculated methane inflow rates were reported as monthly averages.

The mining distances were reported as linear distances mined (including entries and cross cuts), which were around 4500–6500 ft (1372 m–1981 m) per month, rather than the daily advance rate of all three entries in the direction of mine advance as formulated in the model. In order to establish a comparison between measured data and the reservoir model formulation, linear mining distances were converted to net advance of entries. This approach revealed a ratio of 0.27 (1 section length = 3.7 linear length) between these two length scales. Thus, the linear mining distances were converted to distances in the direction of mine advance. The advance rates, using the lengths in the direction of mine advance, were calculated based on two eight-hour production shifts and one maintenance shift per day for 6 days/week. The majority of calculated section advance rates were between 70–110 ft/day (21.3–33.5 m/day) during production shifts and working days. The average rate of mining until both entry sections were developed to full length was approximately 80 ft/day (24.4 m/day).

The Pittsburgh Coalbed generally has a uniform thickness of about 7 ft (2.1 m), although it can vary from 6–8 ft (1.8–2.4 m) in the studied region. These regional variations may affect methane inflow rate into the mine and the methane concentration in the ventilation air. The coalbed thickness information was not included in the data sheet of the monitoring study. Thus, raw tonnages and the average dimensions of the entries and cross cuts were used to convert this information into mining height. The results indicated that the average thickness of the coalbed varied from 6.2–7.6 ft (1.9–2.3 m) in the direction of mining. The

Table 3
Measured (at the monitoring point in return entry shown in Fig. 1) and calculated parameters for mining of tailgate entries

Mining duration from start (months)	Airflow rate (cfm) — measured	Methane concentration (%) — measured	Mining advance rate (ft/day) — calculated	Length of mined entries from start (ft) — calculated	Coal thickness (ft) — calculated
1	44,425	0.250	103	1758	6.9
2	55,533	0.200	100	3468	7.3
3	52,965	0.425	77	4793	7.6
4	60,239	0.500	84	6222	6.9
5	67,850	0.675	42	6939	7.4
6	64,548	0.750	83	8358	6.5
7	64,725	0.925	75	9639	6.2
8	71,280	0.825	98	11,311	6.4

average thicknesses of the coalbed along the tailgate and headgate sections were 6.9 ft and 6.8 ft, respectively.

Changes in reported average methane concentration during monitoring were caused by changes in mining rates, mining height, and ventilation rates. The measured methane concentration in the mine atmosphere increased from 0.25% at the beginning of the headgate and tailgate development to 0.85% at the end. The averages over the entire mining period were 0.56% and 0.57% for tailgate developments and headgate developments, respectively. However, it should be noted that the ventilation airflow increased from 44,000 cfm (ft^3/min) to 70,000 cfm (20.76 m^3/s and 33.04 m^3/s) measured at monitoring points shown in Fig. 1 during this same period (Tables 3 and 4). Although the mine was successful in maintaining methane levels below the 1% statutory limit for the whole mining period, increasing methane concentrations suggest that the increase in methane inflow rate offset the increase in ventilation airflow. To maintain a constant, low methane concentration, the ventilation airflow should have increased as the length of the developed entries increased. Tables 3 and 4 show the measured and calculated parameters discussed above for mining of tailgate and headgate entries in Fig. 1.

4.2. Comparison of reservoir model prediction with in-mine monitoring data

The predictive performance of the reservoir model was compared with in-mine measurements of methane inflow, reported as monthly averages, during development mining of the tailgate and headgate entries. Since there was no report indicating that the area was degasified using horizontal wells, reservoir models developed without the degasification option and their outputs of predicted methane inflow and ventilation airflow rates were compared with the measured data. The reservoir models utilized mining parameters that were close to the calculated averages of monitored variables, i.e., 7 ft (2.1 m) mining height, 70 ft/day and 110 ft/day (21.3 m–30.5 m) advance rate, and 2000–12,000 ft (610–3658 m) development length. Airflow rates were calculated to produce a constant 0.5% methane concentration based on methane inflow predictions.

Fig. 4 shows the simulator predictions and measured methane inflows into the headgate and tailgate entries. The solid markers and the trendlines show the simulator predictions for methane emissions at two different mining rates, upper and lower limits of the calculated average advance rate of the mining, as a function of

Table 4
Measured (at the monitoring point in return entry shown in Fig. 1) and calculated parameters for mining of headgate entries

Mining duration from start (months)	Airflow rate (cfm)-measured	Methane concentration (%) — measured	Mining advance rate (ft/day) — calculated	Length of mined entries from start (ft) — calculated	Coal thickness (ft) — calculated
1	47,830	0.425	80	1360	6.7
2	47,949	0.750	78	2697	6.6
3	45,530	0.475	63	3781	6.3
4	49,445	0.325	20	4131	6.8
5	53,065	0.433	90	5676	7.1
6	43,915	0.600	96	7319	6.7
7	63,540	0.725	89	8848	6.5
8	69,120	0.850	109	10,701	7.6

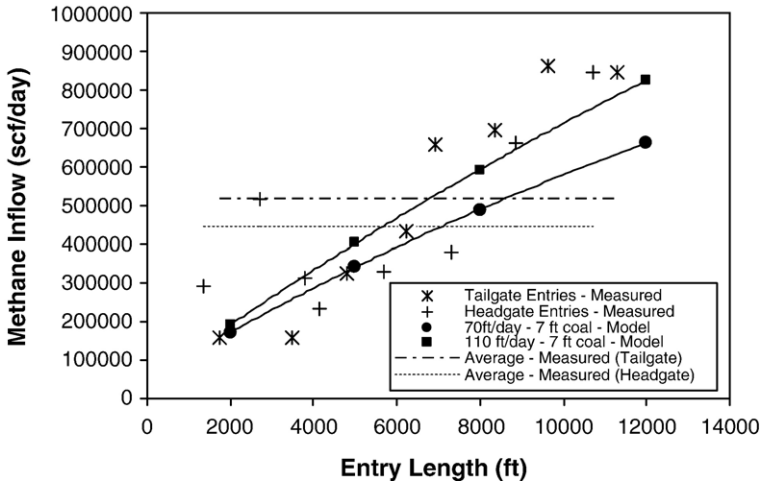

Fig. 4. Comparison of methane inflow calculated in the mine based on measurements of airflow rate and air quality and the simulator predictions at two different mining rates.

entry lengths. Since the simulations use constant mining and coalbed parameters, the methane inflow results show a continuous increase with the length of mined entries, as opposed to the scattered increase in measured data. However, the developed model closely predicts the range of measured data.

The predicted airflow rates needed to maintain a constant 0.5% methane level in the ventilation air and the measured airflow rates that resulted in an average methane concentration of 0.57% are shown in Fig. 5. This figure shows that, because of methane inflow increases, simulator predictions of air requirement increase with entry length to keep the methane levels at 0.5%. Although the average predicted airflow rate is close to the average of the measured values, the measured values at the start and end of the mining are higher and lower than the predicted, respectively. The model calculates the required amount of air based on the simulated methane inflow. During mining, the ventilation air rate was kept in a narrow range regardless of the length of the developed section or the mining rate. In fact, methane levels increased from 0.20% at the beginning of development to 0.85% at the end of development (Tables 3 and 4), indicating an abundance of ventilation air at the beginning and a lack of airflow at the end. This comparison suggests that adjusting airflow quantity based upon mining progress using a predictive method may be safer and more economical than

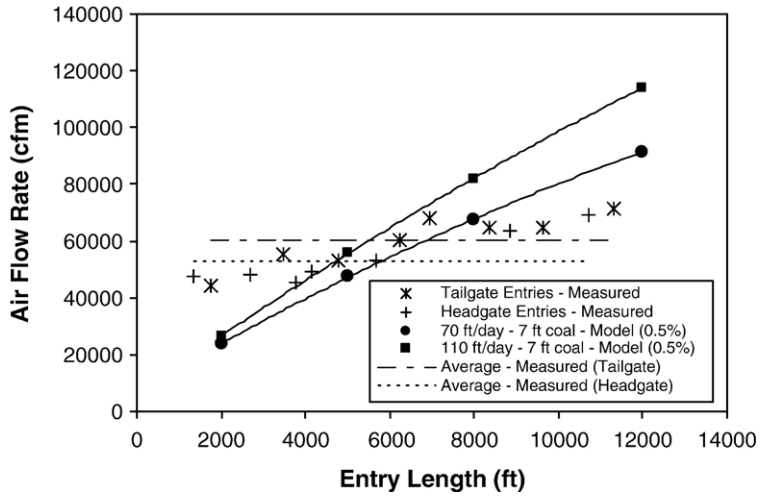

Fig. 5. Comparison of airflow rate measured in the mine and the simulator calculation based on two different mining rates to maintain a constant methane level of 0.5%.

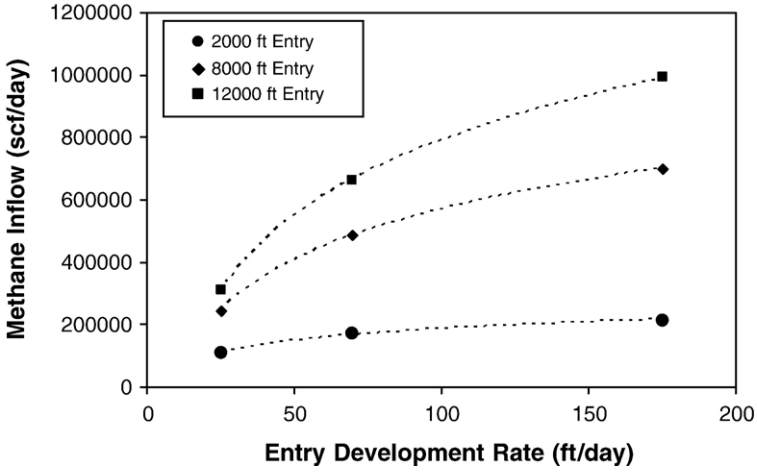

Fig. 6. The change of methane inflow rates predicted by the reservoir simulation as a function of the mining rate for different entry lengths.

supplying a fixed volume of air based on projected maximum demand.

4.3. Parametric analysis of reservoir-modeling results

The reservoir model was used to generate parametric simulations to cover a range of values for the mining-related parameters shown in Table 2. Some of those results, which later were used to develop an artificial neural network (ANN) prediction and optimization tool, are presented in this section to show the relationships and effects of different parameters on methane inflow into the entries during development mining.

The reservoir models predicted the methane inflow rate into the entries. Once the methane inflow rate is known, the airflow requirements can be calculated to keep methane concentrations at a required level. Fig. 6 shows the predicted methane inflow rates at 2000, 8000, and 12,000 ft (610 m, 2438 m, and 3658 m) of roadway development in the 7-ft-high Pittsburgh Coalbed with different development rates. Results show that the methane inflow rate increases with the length of the development section because of the increase in surface area of the exposed coalbed. This increase is a strong function of the mining rate. However, the effect of the mining rate on methane inflow is less pronounced for shorter development distances than longer distances. For 2000 ft of roadway development, increasing the mining rate from 25 ft/day (7.6 m/day) to 175 ft/day (53 m/day) increases the methane inflow rate from 109,100 scf/day (3091 m^3/day) to 214,000 scf/day (6062 m^3/day), which is approximately a two-fold increase. With an 8000 ft entry development, after increasing the mining rate from 25 ft/day to 175 ft/day,

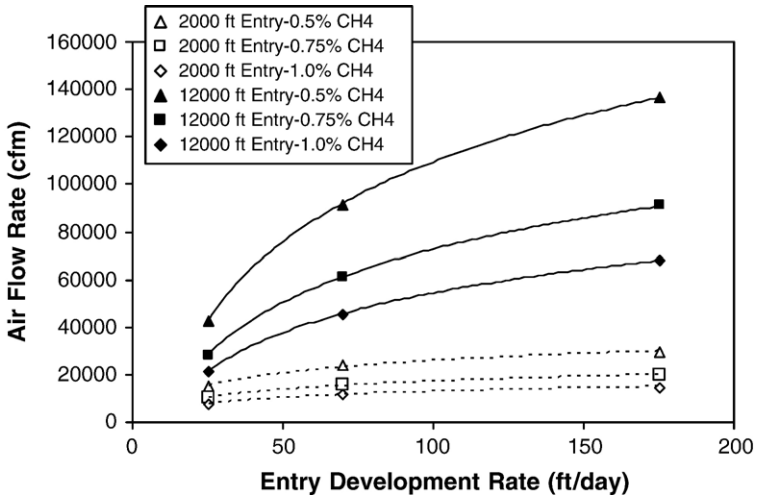

Fig. 7. Calculated airflow rates required to maintain various methane concentrations for different mining rates and entry lengths.

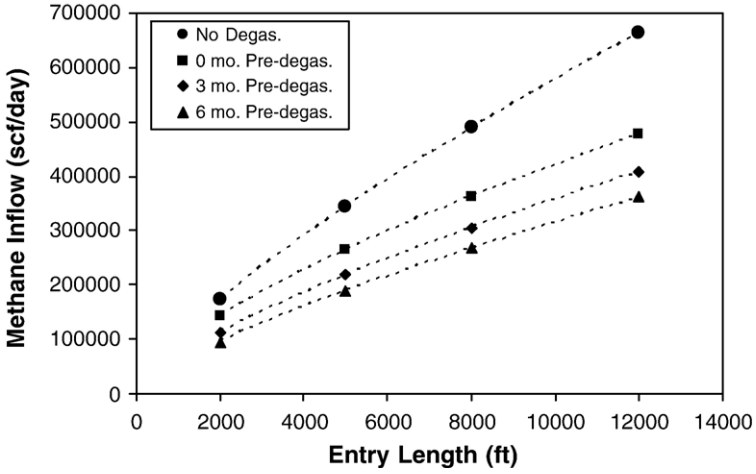

Fig. 8. Methane inflow rate predictions for different development lengths and various pre-mining degasification durations. "No degasification" in the figure legend corresponds to the case where there was no degasification boreholes. On the other hand, 0 months pre-mining degasification and methane production from the wells starts at the same time as the mining. Data represents a development rate of 70 ft/day (21.4 m/day) and horizontal boreholes located 19 ft (5.8 m) from the entries.

the methane inflow increases from 244,300 scf/day (6921 m^3/day) to 700,500 scf/day (19,850 m^3/day). Similarly, increasing the mining rate from 25 ft/day to 175 ft/day in developing 12,000 ft of entries increases methane inflow rate from 309,000 scf/day (8755 m^3/day) to 991,150 scf/day (28,079 m^3/day).

The methane inflow simulations performed for development mining can be used for evaluating and designing ventilation requirements. Fig. 7 shows the calculated airflow requirements as a function of the mining rate to keep methane concentrations at predetermined concentrations during development of 2000 and 12,000 ft (610 m and 3658 m) entry sections. For this calculation, the methane inflow rates shown in Fig. 6 were used. With shorter development distances, only minimal adjustments to ventilation airflow are needed to keep methane levels below 1%. Such adjustments appear to be independent of the mining rate. With longer development distances, more ventilation airflow is needed to keep methane levels constant and the amount is more strongly affected by the mining rate. If the ventilation rate cannot control methane levels, decreasing the mining rate can be considered as a desired control.

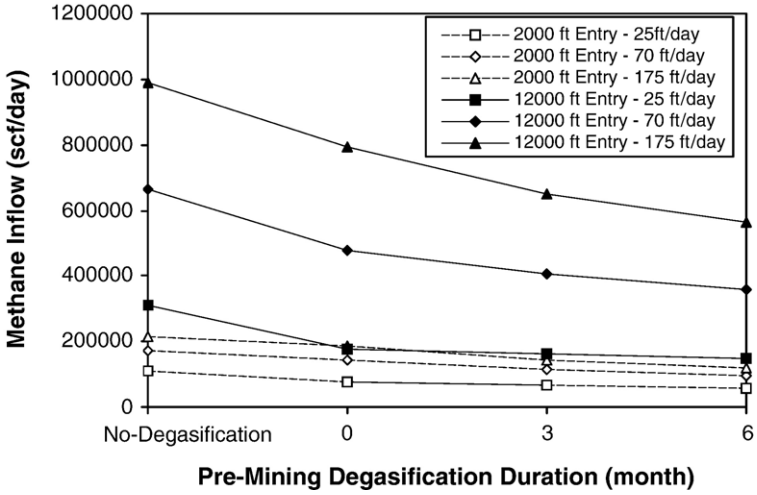

Fig. 9. Effect of degasification duration on the methane inflow rate for various development lengths and rates. "No degasification" in *X*-axis corresponds to the case where there were no degasification boreholes located 19 ft the entries. Different months are the pre-mining degasification durations using boreholes located 19 ft from the entries.

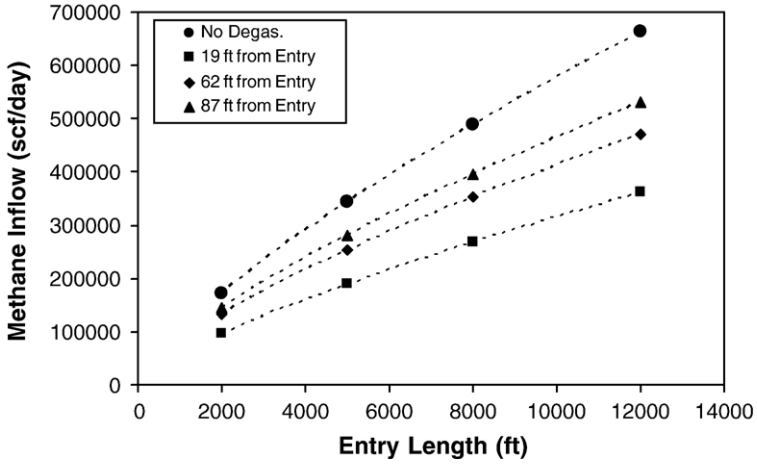

Fig. 10. Effect of proximity of shielding wells to the entries and the length of entries on methane inflow rate. "No degasification" in the figure legend corresponds to the case where there were no any degasification boreholes. The other data are after 6 months of degasification. The simulated data shown is for 70 ft/day (21.4 m/day) development rate.

Using in-seam horizontal boreholes is an effective approach to shield entries against methane inflow during development mining. To simulate the shielding effects of degasification wells on methane inflow and on the ventilation air requirements during development mining, pre-mining degasification periods of 0 months (i.e., no pre-mining degasification) and 3 and 6 months were modeled. The boreholes were placed 19–87 ft (5.8–26.5 m) away from the entries for parametric analysis. In all cases, the wellbores were operated during mining regardless of the duration of pre-mining degasification.

Fig. 8 shows a comparison of methane inflow rates as a function of development length for horizontal boreholes located 19 ft (5.8 m) away from the intake and return entries and operated for various pre-mining durations. The data represents a 70-ft/day (21.4 m/day) development rate in a 7-ft (2.1-m) thick coalbed. Simulations show that the methane emissions are highest when shielding is not used against methane inflow before or during mining. Emission rates progressively decrease as a result of shielding and degasification. For instance, even if the boreholes are not operated before mining and begin to operate when mining starts, the inflow rate decreases about 25% compared to the completely unshielded case. The methane inflow rates after longer pre-mining degasification times are less.

Fig. 9 shows the effect of mining rate and pre-mining degasification duration when mining development

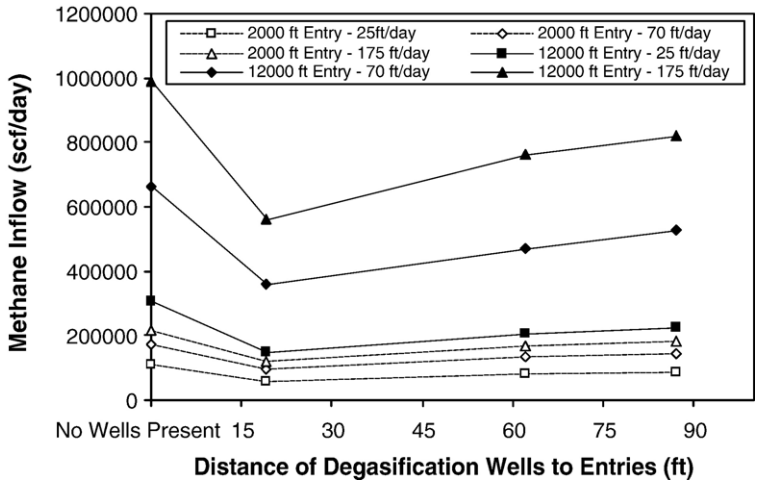

Fig. 11. Effect of mining rate and shielding well proximity when mining 2000-ft and 12,000-ft (610-m and 3658-m) long entries. Wells operated for 6 months prior to the start of development mining.

entries with lengths of 2000 and 12,000 ft (610 m and 3658 m). The presence of methane shielding and the duration of pre-mining degasification are more important when development distances are long and mining rates are high.

Fig. 10 shows the effects of the proximity of the shielding wells to the entries and the development length on methane inflow rate. The simulated data shown is for 70-ft/day (21.4 m/day) development rate in 7-ft (2.1-m) thick coalbed after 6 months of pre-mining degasification, except for the no-degasification case, which does not have any shielding. This figure shows that those wellbores closest to the entries are most effective in reducing methane inflow rates during development mining, about 50% at 12,000 ft (3658 m) compared to no-shielding. Thus, positioning wells as close to the entries as practically possible serves better for shielding purposes.

Fig. 11 shows the effect of mining rate and shielding well proximity for mining 2000-ft and 12000-ft (610-m and 3658-m) long entries after operating the wells for 6 months prior to the start of development mining. Operating shielding wells that are located at close proximity to the entries for 6 months prior to mining may reduce the methane inflow rate into the entries as much as 50% during development mining, especially when mining longer entry sections at higher mining rates.

5. Development and application of artificial neural networks (ANNs) integrated with reservoir simulation as a prediction and optimization tool for development mining

5.1. Basic principles and components of an ANN

A neural network is a computing tool that processes information by its dynamic state response to external inputs (Kosko, 1992). One of the most widely used neural network topologies is the *multilayer perceptron* (MLP) because of its applicability to different problems (Hagan, 1997; Schalkoff, 1997). In MLPs, the minimum number of layers is three, which includes input, hidden, and output layers. Generally, as the problem gets complicated, larger and complex ANN topologies may be required. However, although topologies of this nature generally will achieve mostly lower errors, this may also be due to over-fitting rather than good modeling (Statsoft, 2003).

The total (net) input to a neuron and its output are calculated using a *transfer function*, or *axon*. This is

Table 5
The performance results of different ANN topologies tested to find the suitable network for the development mining simulations without degasification or shielding boreholes

	Hidden layers	Neuron per hidden layer	Epoch	Transfer function	Momentum	Training		*X*-validation		Testing	
						Minimum MSE	Final MSE	Minimum MSE	Final MSE	NMSE	*R*
1	1	4	500	Tanhaxon	0.3	0.00462	0.00462	0.00498	0.00498	0.1892	0.90318
2	1	4	500	Tanhaxon	0.5	0.00499	0.00499	0.00621	0.00621	0.2140	0.89137
3	1	4	500	Tanhaxon	0.7	0.00312	0.00312	0.00286	0.00286	0.1142	0.94237
4	1	6	500	Tanhaxon	0.7	0.00193	0.00193	0.00176	0.00176	0.0599	0.96992
5	1	6	1000	Tanhaxon	0.7	0.00064	0.00064	0.00106	0.00106	0.0184	0.99085
6	1	4	1000	Tanhaxon	0.7	0.00184	0.00184	0.00127	0.00127	0.0656	0.96719
7	1	4	2000	Tanhaxon	0.7	0.00059	0.00059	0.00049	0.00049	0.0206	0.98964
8	**1**	**6**	**2000**	**Tanhaxon**	**0.7**	**0.00029**	**0.00029**	**0.00023**	**0.00023**	**0.0134**	**0.99335**
9	1	6	1500	Tanhaxon	0.7	0.00062	0.00062	0.00056	0.00056	0.0219	0.98899
10	1	6	2000	Tanhaxon	0.8	0.00046	0.00046	0.00043	0.00043	0.0207	0.98970
11	2	6	2000	Tanhaxon	0.7	0.00035	0.00035	0.00034	0.00034	0.0090	0.85549
12	1	4	500	Sigmoid	0.3	0.01201	0.01201	0.01931	0.01931	0.8952	0.68225
13	1	4	500	Sigmoid	0.5	0.01237	0.01237	0.02040	0.02040	0.9292	0.77537
14	1	4	500	Sigmoid	0.7	0.01003	0.01003	0.01681	0.01681	0.7764	0.80288
15	1	6	500	Sigmoid	0.7	0.00574	0.00574	0.00961	0.00961	0.4895	0.85107
16	1	6	1000	Sigmoid	0.7	0.00407	0.00407	0.00666	0.00066	0.3812	0.84414
17	1	4	1000	Sigmoid	0.7	0.00558	0.00558	0.00937	0.00937	0.4694	0.83881
18	1	4	2000	Sigmoid	0.7	0.00202	0.00202	0.00263	0.00263	0.2690	0.85800
19	**1**	**6**	**2000**	**Sigmoid**	**0.7**	**0.00171**	**0.00171**	**0.00198**	**0.00198**	**0.2414**	**0.87429**
20	1	6	4000	Sigmoid	0.7	0.00153	0.00153	0.00167	0.00167	0.2253	0.88322
21	2	6	2000	Sigmoid	0.7	0.01249	0.01249	0.02061	0.02061	0.9434	0.81673

Data rendered in bold are the most suitable topologies in each category, among the schemes tested. All the learning rules are momentum.

sometimes called a "squashing function" (Eberhart and Dobbins, 1990), since it compresses the output range between either 0 to1 or −1 to 1, depending on the choice of the transfer function. While there are various transfer functions, the *hyperbolic tangent axon* (Tanhaxon) and *Sigmoid functions* are generally the non-linear axons used.

Based on the training method, neural networks are classified as either supervised or unsupervised networks (Mohaghegh, 2000). The supervised training algorithm requires repeated showings (Epoch) of both input vectors and the expected outputs of the training set to the network to let it learn the relations on a feedback basis (Gorucu et al. 2005). The neural network computes its output at each epoch and compares it with the expected output (target) of each input vector in order to calculate the error. Minimizing the mean square error (MSE) is the goal of the training process. The most widely used technique is to propagate the error back and adjust the initially assigned random weights to each neuron. This process is called back-propagation. This is the technique used in the modeling described in this paper. Training is one of the most important steps in the development phase of the neural network, since the weights and the network characteristics will be used later in testing data sets and making subsequent predictions.

Cross validation and testing are the performance measures of the network with new data that give confidence that the network is able to recognize the training patterns and generalize the relationships, within a certain degree of acceptable error.

5.2. Reservoir simulations as the source of the input–output patterns

The "dynamic" reservoir simulation model that predicted the methane inflows generated "synthetic" case studies to develop an artificial neural network-based prediction and optimization tool. Airflow requirements

Table 6
The performance results of different ANN topologies tested to find the suitable network for the development mining simulations with degasification/shielding boreholes

	Hidden layers	Neuron per hidden layer	Epoch	Transfer function	Momentum	Training		*X*-validation		Testing	
						Minimum MSE	Final MSE	Minimum MSE	Final MSE	NMSE	*R*
1	1	4	500	Tanhaxon	0.3	0.00412	0.00412	0.00567	0.00567	0.13408	0.93107
2	1	4	500	Tanhaxon	0.5	0.00351	0.00351	0.00518	0.00518	0.11492	0.94124
3	1	4	500	Tanhaxon	0.7	0.00332	0.00332	0.00490	0.00490	0.10858	0.94475
4	1	6	500	Tanhaxon	0.7	0.00211	0.00211	0.00289	0.00289	0.06592	0.96733
5	1	8	500	Tanhaxon	0.7	0.00304	0.00304	0.00469	0.00469	0.10479	0.94635
6	1	6	1000	Tanhaxon	0.7	0.00073	0.00073	0.00113	0.00113	0.03076	0.98499
7	1	6	2000	Tanhaxon	0.7	0.00052	0.00052	0.00085	0.00085	0.02452	0.98845
8	1	6	1500	Tanhaxon	0.7	0.00051	0.00051	0.00074	0.00074	0.02174	0.98990
9	1	8	2000	Tanhaxon	0.7	0.00282	0.00282	0.00457	0.00457	0.09693	0.95086
10	**1**	**8**	**2000**	**Tanhaxon**	**0.8**	**0.00034**	**0.00034**	**0.00059**	**0.00059**	**0.01170**	**0.99420**
11	1	10	2000	Tanhaxon	0.8	0.00030	0.00030	0.00075	0.00075	0.02005	0.99069
12	1	10	2000	Tanhaxon	0.7	0.00034	0.00034	0.00067	0.00067	0.01933	0.99095
13	1	10	1500	Tanhaxon	0.7	0.00075	0.00075	0.00082	0.00082	0.01880	0.99108
14	1	8	4000	Tanhaxon	0.7	0.00034	0.00034	0.00073	0.00073	0.02162	0.98959
15	2	6	1500	Tanhaxon	0.7	0.00076	0.00076	0.00115	0.00115	0.03222	0.98523
16	1	4	500	Sigmoid	0.3	0.01524	0.01524	0.01171	0.01171	0.95764	0.61147
17	1	4	500	Sigmoid	0.5	0.01567	0.01567	0.01213	0.01213	0.94738	0.80786
18	1	4	500	Sigmoid	0.7	0.01186	0.01186	0.00900	0.00900	0.73909	0.85221
19	1	6	500	Sigmoid	0.7	0.00899	0.00899	0.00657	0.00657	0.55004	0.86702
20	1	8	500	Sigmoid	0.7	0.00904	0.00903	0.00685	0.00685	0.57277	0.85524
21	1	6	1000	Sigmoid	0.7	0.00467	0.00467	0.00356	0.00356	0.29142	0.89142
22	**1**	**6**	**2000**	**Sigmoid**	**0.7**	**0.00221**	**0.00221**	**0.00184**	**0.00184**	**0.14768**	**0.92487**
23	1	8	2000	Sigmoid	0.7	0.00230	0.00230	0.00188	0.00188	0.15540	0.92245
24	1	10	1500	Sigmoid	0.7	0.00258	0.00258	0.00211	0.00211	0.17099	0.91194
25	1	6	1500	Sigmoid	0.7	0.00255	0.00255	0.00211	0.00211	0.17074	0.91233
26	1	6	4000	Sigmoid	0.7	0.00192	0.00192	0.00159	0.00159	0.12652	0.93538
27	2	6	2000	Sigmoid	0.7	0.01506	0.01506	0.01157	0.01157	0.91014	0.83561

Data rendered in bold are the most suitable topologies in each category among the schemes tested. All the learning rules are momentum.

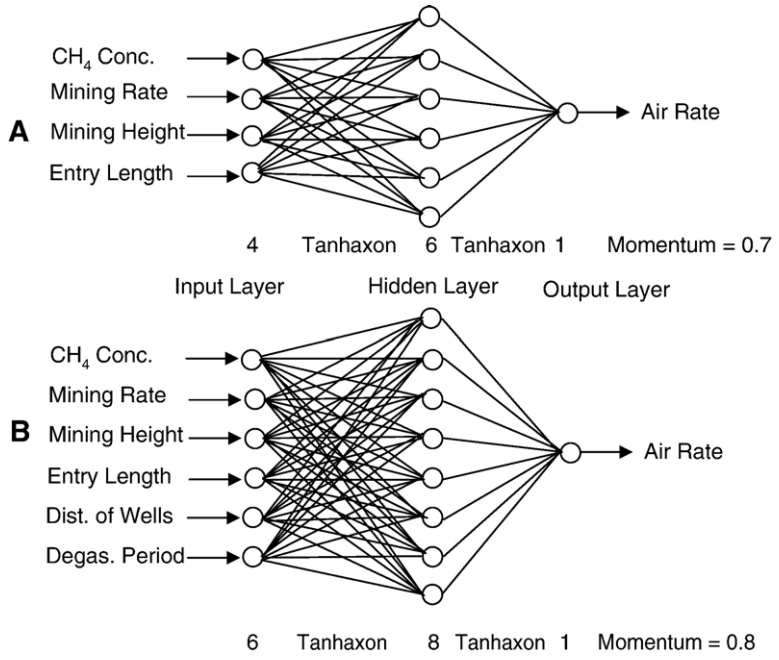

Fig. 12. The ANN topologies developed for two different classes of reservoir simulation for the mine ventilation problems studied in the paper. (A) Prediction of air requirements for ventilating development entries in the absence of any methane degasification and shielding around the entries. (B) Prediction of air requirements in the presence of degasification and the shielding against methane inflow).

were calculated for required methane concentrations based on methane inflows predicted by the reservoir simulation.

For the purposes of developing an ANN tool and training it as a predictive tool, the reservoir simulation results were divided into two groups based on the use of degasification. The reservoir simulations without degasification resulted in four variables, each with its own range of values, and reservoir simulations with the degasification option resulted in six variables, shown in Table 2. The values of the input variables were changed between model runs to create physically meaningful simulation data points. Therefore, 360 modeling data points (exemplars) for the no-degasification case and 720 exemplars for the degasification case were generated for these two classes of simulations.

5.3. Development of ANN models

The development and implementation of the ANN were performed using NeuroSolutions™ version 5.0 software (NeuroDimensions, 2006). Entry developments with and without degasification were considered separately with two different ANNs constructed for each case. The whole data set (exemplars) created for each class of problem was separated into three sections to use them for training, cross validation, and testing purposes. In the case of simulations without shielding boreholes, 252 out of 360 exemplars (70%) were saved as training data, 36 exemplars (10%) were saved as cross-validation data set, and 72 exemplars (20%) were saved for testing the trained network. In the case of the simulations with shielding wells, the number of exemplars separated for training were 288 out of 720 (40%), 144 (20%) for cross validation, and 288 (40%) for testing. The criterion in breaking up the data was to allocate enough exemplars for the ANN training and testing.

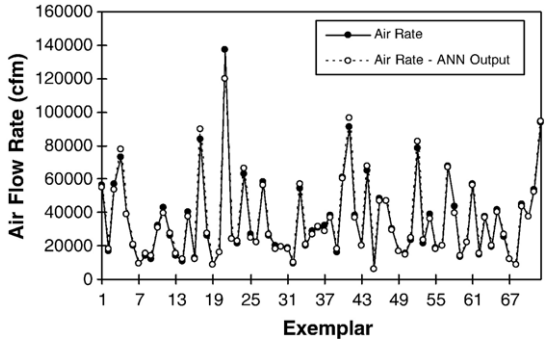

Fig. 13. Comparison of target airflow rates (simulator-based predictions for the case without degasification wells) of the testing data set with the predicted rates from the proposed ANN shown in Fig. 12A.

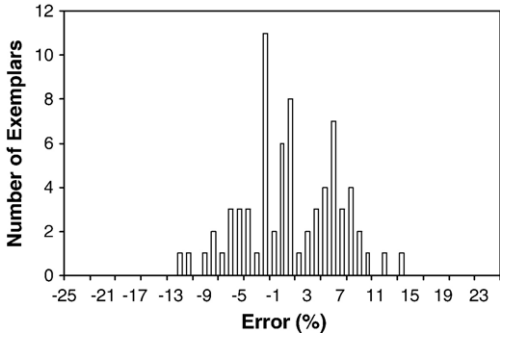

Fig. 14. Distribution of the number of exemplars within certain relative error bins in testing of the completely new data (testing set) for the case without degasification wells (Fig. 13) using the network in Fig. 12A.

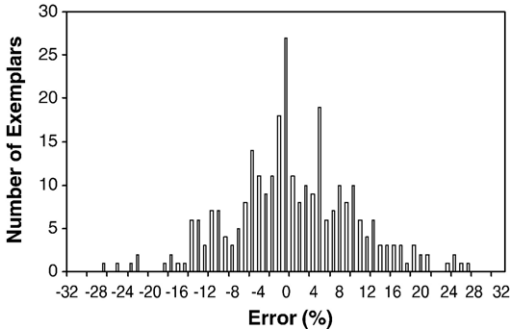

Fig. 16. Distribution of the number of exemplars within certain relative error bins in testing of the completely new data (testing set) for the case without degasification wells (Fig. 15) using the network in Fig. 12B.

5.3.1. Performance study for the selection of a suitable ANN topology

In order to determine an appropriate ANN topology and to identify network parameters for training and testing, various combinations of parameters were tested. Values of minimum and final mean squared error (MSE) were noted for training and cross validation of the ANN. Also, values of nominal mean squared error (NMSE), regression coefficient, and absolute error were noted for testing the ANN. The number of hidden layers, the number of neurons in hidden layers, the number of epochs, the type of transfer function, and the value of momentum were varied. Tables 5 and 6 give the results of this parametric search to build an ANN for the analyzed ventilation problems.

Table 5 gives the results of the parametric search for a suitable network structure function for the ventilation of entries in the absence of degasification. In this sensitivity study, a single-hidden layer was predicted to be adequate, although one case with two hidden layers was tested as well. The best combination of network topology and parameter values were obtained with 6 neurons, 2000 epochs, and 0.7 as the momentum value using a tanhaxon transfer function. The MSEs obtained in the training and cross-validation phases (0.00029 and 0.00023, respectively), and the NMSE and R (0.0134 and 0.993, respectively) were the best combinations among the examined networks. The minimum and maximum absolute errors were 10.3 ft^3/min (cfm) (0.00486 m^3/s) and 17,400 cfm (8.21 m^3/s), respectively. Sigmoid function was also tested with several combinations of parameters, but its results were not as good as the ones obtained with tanhaxon transfer function (Table 5).

A similar sensitivity analysis was performed with the data set using the shielding option. Table 6 gives the results of performances achieved with various combinations of network topology and tested parameters. In this analysis, 1 hidden layer, 8 hidden-layer neurons, 2000 epochs, and a momentum value of 0.8 gave the best results for the tanhaxon transfer function tests. This combination gave low MSEs in training and in cross-

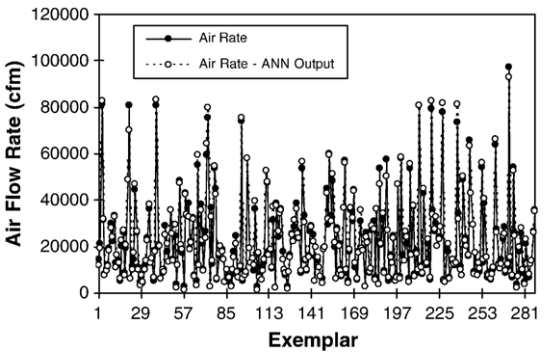

Fig. 15. Comparison of target airflow rates (simulator-based predictions for the case without degasification wells) of the testing data set with the predicted rates from the proposed ANN shown in Fig. 12B.

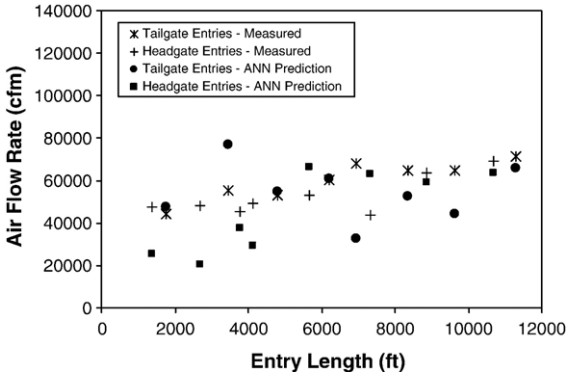

Fig. 17. Comparison of monthly-averaged airflow rate measured during development of tailgate and headgate entries shown in Fig. 1 and the ANN predictions based on the calculated input parameters.

validation runs (0.00034 and 0.00059, respectively), a low nominal mean squared error (0.0117), and a high regression coefficient in the testing phase (0.9942). The minimum and maximum errors were 4.39 cfm (0.00207 m^3/s) and 10,700 cfm (5.29 m^3/s), respectively. Although higher numbers of hidden-layer neurons (10) were tested with both 0.7 and 0.8 momentum coefficients, the results did not improve. The Sigmoid function performed less efficiently than the tanhaxon function for every combination tested (Table 6). Thus, the tanhaxon was selected as the transfer function for the ANN network to analyze ventilation with degasification.

The topologies shown in Fig. 12 are proposed as a tool to analyze and predict ventilation airflow requirements with and without the use of degasification.

5.3.2. Training of the ANN models

Ventilation of underground coal mines is a complex process and involves many considerations since the methane gas levels may change. Some of these factors include reservoir properties of the coalbed, mining operation-related changes in the methane inflow into the entries, the length of development entries, and the presence or absence of any previous degasification or shielding. In this study, changes in the reservoir properties of the coalbed were excluded from the variables, by adapting the models for the Pittsburgh Coalbed. Even then, it is not easy to predict an optimized ventilation airflow rate to achieve a certain methane level for the three-entry mine geometry shown in Figs. 1–3. In the absence of a data library and an appropriate tool to analyze it, the only choice is to create and run a new reservoir model, which usually is a lengthy process. While it is also possible to make some estimates based on interpolations, that approach is not only time consuming but is usually inaccurate. Ultimately, the ANN is expected to make accurate estimates for completely new input parameters, by reproducing the results of these simulations and approximating the results of a completely new data set.

For training and cross validation of the ANN shown in Fig. 12A, developed for the case without degasification, 252 training patterns and 36 cross-validation patterns were shown to the network 2000 times (epoch) to establish the relationships and minimize the error. The MSE for training and cross validation of this network as a function of the epoch showed that the error began to decrease rapidly for both training and cross validation. However, the minimum MSEs were obtained at the end of the 2000 epoch cycles. The final MSEs obtained were 0.00029 and 0.00023 for training and cross validation, respectively.

For training and cross validation of the ANN developed for the case with degasification (Fig. 12B), 288 training patterns and 144 cross-validation patterns were shown to the network 2000 times as determined from the ANN performance study (Table 6). The tanhaxon was selected as the transfer function and 0.8 was used as the momentum factor for this network having one hidden layer, eight hidden neurons, and six input neurons. For this network, the minimum and also final MSEs obtained at the end of the 2000th epoch cycle were 0.00034 for training and 0.00059 for cross validation.

5.3.3. Testing of the developed ANN models

The trained networks were tested in two stages. In the first stage, the networks were tested using the training data. The same training data set was presented to the network in the testing phase to note the prediction performance. In the second stage of testing, the ANN was exposed to a new data set (testing set) that it had not yet seen. This is an important test to see if the ANN generates acceptable predictions for the new data patterns or, in other words, to see whether it recognizes the patterns and generalizes the results with which it was trained. In some cases, a trained network may give close predictions to the training set when the same data is used in the testing phase. Poor predictive performance towards a new set suggests that the ANN cannot generalize or recognize patterns and this may indicate memorization. Therefore, two-stage testing should give an idea about the performance and thus predictive capability of the trained ANNs.

In testing of the ANN model without shielding boreholes (Fig. 12A), the performance of the network was first tested against the training data set having 252 exemplars. The analysis showed that the airflow rates predicted by the network were very close to the target values (simulator-based predictions) in the training set for the majority of the data set. The minimum and maximum absolute errors were 1.20 cfm (0.00056 m^3/s) and 10250 cfm (4.84 m^3/s), respectively. The NMSE and R values were 0.0043 and 0.9978, respectively, which shows a good degree of success in the prediction performance. Using training data set in testing, the prediction errors revealed that the error generally fluctuated between +/−5% depending on the airflow rate variations between predictions and targets, although it is generally less than 5% for most of the data set. Distribution of exemplars within certain error bins revealed that the error for 50 of the exemplars (19.7%) was between +/−1%. The number of exemplars having +/−3% error was 129 (51%) in the data set. When an

error margin of +/−5% was considered, 183 (72%) exemplars fell within this range. Overall, 91% of the data had an error less than 10%. The average of the absolute value of relative errors for the entire set of exemplars was 4.0%.

In the second stage of testing for this ANN (Fig. 12A), the network was exposed to a new data set (testing set) to evaluate its predictive performance. For this simulation, 72 exemplars were saved. Fig. 13 shows the comparison of airflow rates predicted by the network to the target values of the testing set calculated by the reservoir simulator. This figure shows that the predictions of the trained network are close to the simulator predictions for the completely new data set. For testing with this new data set, the NMSE and *R* values were 0.0134 and 0.993, respectively. The minimum and maximum absolute errors in airflow rate predictions were 10.3 cfm (0.00485 m^3/s) and 17,400 cfm (8.21 m^3/s). The number of exemplars within different relative error bins shows that the number of exemplars with +/−3% error is 30, or 42% of all data (Fig. 14). For 85% of the exemplars, the error is less than +/−8%. The average absolute value of relative error of prediction for the whole set of exemplars is 4.39%. These results suggest that the network in Fig. 13 is capable of making reasonably accurate predictions for a new data set. This network also looks very promising for predicting ventilation airflow rates for development mining.

In testing of the ANN in the presence of shielding boreholes (Fig. 12B), the same procedure was applied. ANN learning was tested against the training data set. For this process, a training data set with 288 exemplars was introduced to the network as the testing, or "new," data set. This analysis showed that the predicted values were close to the target values of the data set. The nominal MSE and *R* values were 0.0076 and 0.9962, respectively. The low error and high correlation coefficient are good indicators of predictive performance. The minimum and maximum absolute errors in airflow rates for the predictions were 11.4 cfm (0.00537 m^3/s) and 10920 cfm (5.15 m^3/s), respectively. In this phase, the relative errors using the predicted and target airflow rates showed that the error fluctuated within a narrow band. For most of the exemplars, the error was +/−10%. The average of the absolute values of the relative errors was 7.0%. The distribution of exemplars within different error bins shows that 137 (48%) of all exemplars had a relative error +/−5%. The number of exemplars with less than +/−10% relative error was 222 (77%). For a +/−15% error range, the number of exemplars within this range of error was 258, or 89% of all data.

In the second stage, the performance of this ANN (Fig. 12B) was assessed with a new data set containing 288 exemplars (testing set). The result indicated reasonably good predictive capability for the new data set and show that the network can recognize and generalize patterns of input data. The minimum and maximum absolute errors between predictions and targets are 4.4 cfm (0.002 m^3/s) and 10,660 cfm (5.03 m^3/s), respectively with an NMSE of 0.00117 and an *R* value of 0.9942 (Fig. 15). The error histogram in Fig. 16 shows that 85 of the exemplars (30% of the entire set) and 133 of the exemplars (46% of the set) have less than +/−3 and +/−5% error, respectively. This data also shows 208 exemplars (72%) with +/−10% error and 27 exemplars (9%) with an error of +/−15% or more.

The comparison of ANN predictions for the airflow rates and the error analyses show that the proposed ANNs perform reasonably well for the prediction and optimization of ventilation air requirements. The flexibility and predictive capability of trained ANNs offer advantages in decision making and design processes.

5.4. Comparison of airflow rate predictions of the trained ANN with the in-mine measurements

The trained ANN without shielding boreholes predicted ventilation airflow rates during development of tailgate and headgate entries shown in Fig. 1. Fig. 17 shows the measured airflow rates, reported as monthly averages, and the predicted airflow rates using the trained ANN shown in Fig. 12B. The following input data (Tables 3 and 4) was collected and used by the ANN to predict airflow rates: monthly average methane concentration data measured in the mine, calculated mining advance rates using reported monthly linear mining distances, calculated average mining height using reported monthly coal production tonnages and the dimensions of the entries, and the calculated entry length based on the monthly linear footage mined. As shown in Fig. 17, the predictions of the trained ANN are generally in good agreement with the field data. There are a few data points that show relatively high error compared to others, which may have arisen from the calculated parameters that may have been different from their actual field values.

Unfortunately, the predictions of the ANN with shielding boreholes could not be compared with in-mine measurements because of the absence of reported data. However, it would be reasonable to expect acceptable agreement with predictions and field data. One of the advantages of developing ANNs in conjunction with realistic simulations is that it increases the predictive

versatility of the ANN when other data sources are limited.

Although the reservoir and the ANN models for development mining were based on Pittsburgh Coalbed parameters, the values of the coalbed reservoir properties may be varied in the parametric reservoir simulations. Developing and training potentially larger ANN models would enable the mining and the coalbed parameters to be generalized for operations in other coal regions.

6. Summary and conclusions

This study presented the development and application of "dynamic" reservoir models and artificial neural networks to predict and optimize methane inflows and ventilation airflow requirements for development mining of coal seams. The reservoir models were developed for a typical three-entry system practiced in the Northern Appalachian Basin section of the Pittsburgh Coalbed. These models considered the presence and absence of boreholes against methane inflow. Model simulations were performed by changing various mining and degasification parameters in a systematic manner to predict methane inflows and airflow requirements. The reservoir model predictions were compared with the in-mine measurements available from the mining of tailgate and headgate entries around a longwall panel in the Pittsburgh Coalbed.

The predictions from the reservoir simulations were used to develop, train, and test the artificial neural networks (ANNs). Various network structures were tested to evaluate the predictive capabilities of the ANN. The ANN predictions were compared with the reservoir simulation results and the resulting prediction errors were evaluated. Finally, the ANN was asked to predict the airflow rates measured in the entries of the Pittsburgh Coalbed mine using reported and calculated mining parameters.

This study made the following conclusions:

1. Reservoir simulation can be used effectively for modeling development mining in underground coal mines. It can predict methane inflows into the entries based on various coalbed and operating parameters, from which the ventilation airflow requirements can be predicted to maintain a desired methane level.
2. Methane inflow rate increases with entry length because of increases in the surface area of the coalbed exposed to the mine environment. These increases are a logarithmic function of the mining rate. However, the effect of the mining rate is less pronounced on methane inflow for shorter development distances compared to longer development distances.
3. For shorter development distances, marginal adjustments in ventilation airflow may be adequate to keep methane levels under 1%. The model showed that this adjustment was generally independent of the mining rate. However, longer developments require significantly more ventilation air capacity to keep methane levels constant. This amount is a function of the mining rate.
4. Employing shielding boreholes to protect entries from methane migration during mining is an effective approach. Even if the boreholes cannot be operated for a long time prior to the start of mining, their presence during mining makes a big difference (about 25%) in methane inflow rates, especially during mining of longer sections.
5. Positioning of boreholes relative to entries is important. These results show that positioning wellbores as close to the entries as practically possible is more effective, especially when mining long developments at higher mining rates.
6. Parametric and realistic reservoir simulations can develop, train, and test ANN-based prediction and optimization models, where actual field data is unavailable. The ANNs developed in this study can generate the reservoir simulation data with a reasonable accuracy for predicting ventilation air requirements during development mining.
7. ANN predictions of in-mine measured airflow data were successful when using calculated monthly-averaged input parameters for predictions rather than the spatio-temporal data.
8. The ANN can be generalized to other coalbeds by using parametric reservoir simulations to define the impacts of different coalbed parameters on airflow requirements and methane inflows.

References

Brunner, D.J., Schwoebel, J.J., Li, J., 1997. Simulation based degasification system design for the Shihao Mine of the Songzao coal mining administration in Sichuan China. Proc. 6th International Mine Ventilation Congress, Pittsburgh, PA, pp. 429–433.

Computer Modeling Group Ltd., 2003. Generalized Equation of State Model-GEM. Calgary, Alberta, Canada.

Diamond, W.P., 1994. Methane control for underground coal mines. Information Circular No. 9395, US Dept. of Interior, US Bureau of Mines.

Diamond, W.P., La Scola, J.C., Hyman, D.M., 1986. Results of direct-method determination of the gas content of the U.S. coalbeds. Information Circular No. 9067, US Dept. of Interior, US Bureau of Mines.

Eberhart, R.C., Dobbins, R.W., 1990. Neural Network PC Tools: A Practical Guide. Academic Press Inc., San Diego, CA.

Ertekin, T., Sung, W., Schwerer, F.C., 1988. Production performance analysis of horizontal drainage wells for the degasification of coal seams. Journal of Petroleum Technology 625–631.

Gorucu, F.B., Ertekin, T., Bromhal, G., Smith, D., Sams, N., Jikich, S., 2005. Development of a neuro-simulation tool for coalbed methane recovery and CO_2 sequestration. 2005 International Coalbed Methane Symposium, Tuscaloosa, AL. Paper 0505.

Hagan, M.T., Demuth, H.B., Beale, M.H., 1997. Neural Network Design. PWS Publishing, Boston, MA.

Hardcastle, S.G., Dayss, A., Leung, E., 1997. Integrated mine ventilation management system. Proceedings of 6th International Mine Ventilation Congress. Pittsburgh, PA.

Karacan, C.Ö., Diamond, W.P., Esterhuizen, G.S., Schatzel, S.J., 2005. Numerical analysis of the impact of longwall panel width on methane emissions and performance of gob gas ventholes. 2005 International Coalbed Methane Symposium. Tuscaloosa, AL. Paper 0505.

Karacan, C.Ö., Esterhuizen, G.S., Schatzel, S.J., Diamond, W.P., (in press). Reservoir simulation-based modeling for characterizing longwall methane emissions and gob gas venthole production. International Journal of Coal Geology.

King, G., Ertekin, T., 1991. State of the art modeling for unconventional gas recovery. SPE Formation Evaluation 63–72 (March).

Kosko, B., 1992. Neural Networks and Fuzzy Systems: A Dynamical Systems Approach to Machine Intelligence. Prentice-Hall, Inc., Englewood Cliffs, NJ.

Mohaghegh, S., 2000. Virtual-intelligence applications in petroleum engineering: Part 1-Artificial neural networks. Journal of Petroleum Technology 52 (9), 64–73.

NeuroDimension, 2006. NeuroSolutions 5.0.Gainesville. FL.

Noack, K., 1998. Control of gas emissions in underground coal mines. International Journal of Coal Geology 35, 57–82.

Schalkoff, R.J., 1997. Artificial Neural Networks. McGraw-Hill, New York.

Statsoft., 2003. Neural Networks. http://www.statsoftinc.com/textbook/stneunet.html.

Thakur, P.C., Davis, J.G., 1977. How to plan for methane control in underground coal mines. Mining Engineering 41–45 (October).

Thakur, P.C., Poundstone, W.N., 1980. Horizontal drilling technology for advance degasification. Mining Engineering 676–680 (June).

Thakur, P.C., 1997. Methane drainage from gassy mines—a global review. Proc. 6th International Mine Ventilation Congress. Pittsburgh, PA, pp. 415–422.

Young, G.B.C., Paul, G.W., Saulsberry, J.L., Schraufnagel, R.A., 1993. A simulation-based analysis of multiseam coalbed well completions. 68th Society of Petroleum Engineers Annual Technical Conference and Exhibition. Paper No 26628.

Zuber, M.D., 1997. Application of coalbed methane reservoir simulators for estimation of methane emissions in longwall mining. 6th International Mine Ventilation Congress. Pittsburgh, PA, pp. 436–440.

Zuber, M.D., 1998. Production characteristics and reservoir analysis of coalbed methane reservoirs. International Journal of Coal Geology 38, 27–45.